Available online at www.sciencedirect.com
ScienceDirect
Ceramics International 35 (2009) 3067–3072
CERAMICS INTERNATIONAL
www.elsevier.com/locate/ceramint

Characterization of Al-doped ZnO thermoelectric materials prepared by RF plasma powder processing and hot press sintering

H. Cheng, X.J. Xu, H.H. Hng *, J. Ma

School of Materials Science and Engineering, Nanyang Technological University, Nanyang Avenue, Singapore 639798, Singapore

Received 26 February 2009; received in revised form 8 March 2009; accepted 12 April 2009
Available online 21 May 2009

Abstract

RF plasma processing technique was used to prepare Al-doped (up to 4 at%) ZnO nanopowders. The as-prepared powders were subsequently hot pressed to form sintered pellets. The temperature-dependent electrical and thermal properties of the sintered materials were measured from room temperature to 800 °C. All the doped samples showed metallic electrical conductivity and the overall thermoelectric performances were comparable to doped ZnO thermoelectric materials obtained by other nanoprocessing techniques. The results showed that RF plasma processing technique can be effectively used to produce doped nanopowders. The thermoelectric performance of the doped samples was discussed and related to the microstructure of the materials.

Keywords: C. Electrical properties; C. Thermal properties; D. ZnO; Thermoelectric properties

1. Introduction

Materials and technology capable of providing alternative clean energy are of great research importance. Thermoelectric (TE) materials are attracting renewed attention due to their potential of harvesting huge amount of waste heat from power plant and engine exhaust. In particular, oxide TE materials, being non-toxic, thermally stable and highly resistive to oxidation [1], are good candidates for the energy conversion applications.

Besides the continuous effort to search for new promising TE materials (e.g. p-type layered cobalt oxides Na_xCoO_2 and $Ca_3Co_4O_9$) [2], many attempts have also been made to improve the performance of existing TE materials through novel microstructural and compositional design [3,4]. Recent research predicted that the dimensionless figure of merit, ZT (defined as $(S^2\sigma/\kappa)T$, where S is the thermopower or Seebeck coefficient, σ the electrical conductivity, T the absolute temperature in Kelvins, and κ the total thermal conductivity) of low dimensional nanosized TE materials (e.g. nanoparticles and nanowires) can be significantly improved due to quantum confinement effect and unique band structure [5]. Various processing methods, such as mechanical alloying, sol–gel and polymerized complex synthesis methods have been used to produce nanostructured oxide TE materials [4,6–8].

Currently, reasonably high ZT is only found in p-type oxide TE materials. The progress in developing n-type oxide TE materials with comparable ZT is still lacking, which calls for more research effort in this area. Doped ZnO, especially Al-doped ZnO, is still one of the best n-type oxides TE materials reported to date.

In this work, we attempt to use RF plasma powder processing technique to prepare Al-doped ZnO nanopowders. The potential of using this technique to prepare doped nanopowders will be investigated. It can provide an alternative and promising way to dope element which is difficult to dope through wet chemical processing route. This is also a relatively clean technique as compared to methods such as mechanical alloying where contamination from milling balls is inevitable. The as-prepared powders will be subsequently hot pressed, and the electrical, thermal and thermoelectric properties of the hot-pressed samples will be investigated and discussed.

2. Experimental procedures

An induction RF Plasma System (TEKNA Plasma Systems Inc., Canada) was used in this work. ZnO (99.9%, Aldrich) and

* Corresponding author. Tel.: +65 67904140; fax: +65 67909081.
E-mail address: ASHHHng@ntu.edu.sg (H.H. Hng).

0272-8842/$36.00
doi:10.1016/j.ceramint.2009.04.010

TM-DAR α-Al_2O_3 (99.99%, Taimei Chemical Co. Ltd., Japan) powders were used as starting materials. Aqueous (instead of organic) suspension of the oxide powders was used to avoid carbonized contamination in the sintered samples. Aqueous suspension mixtures with 10 wt.% powder loading were then fed into the plasma chamber by a peristaltic pump. A RF power of 21 kW and an argon pressure of 400 Torr were used throughout the experiment. Fig. 1 shows a schematic view of the TEKNA RF Plasma Systems. The powder containing suspension solutions were sprayed through a stainless steel nozzle into the plasma flame, where the powders were rapidly evaporated and then condensed on the cold wall of the collecting chambers. Powders from chambers C2 and C3 were collected, washed, compacted and sintered using hot press (Centorr Vacuum Industries, USA) at 950 °C for 2 h under pressure of 50 MPa.

The particle size of the raw and as-prepared powders was measured using a ZetaPlus particle size analyzer (Brookhaven instrument, USA). A JSM-6340F (JEOL, Japan) field emission scanning electron microscope (FESEM) and Shimadzu 6000 (Shimadzu, Japan) X-ray diffractometer (XRD) were used to study the microstructure and phase composition of the powders and sintered samples. In order to observe the grain structures, the sintered samples were thermally etched at 900 °C in air for 40 min.

The thermal diffusivity of the sintered samples was measured by a LFA 427 laser flash measurement system (NETZSCH, Germany) in Argon atmosphere. The heat capacity (Cp) measurement was done in a DSC 404 differential scanning calorimeter (NETZSCH, Germany) using nitrogen as the working gas. The electrical and thermoelectric properties were determined using a ZEM-3 power conversion efficiency measuring instrument (ULVAC-RIKO, Japan) in helium atmosphere.

3. Results and discussion

Fig. 2(a)–(e) shows the morphology of the raw ZnO and Al_2O_3 powders together with the Al-doped ZnO powders prepared by plasma processing. Similar morphology was found in both the raw and doped ZnO powders. A bimodal particle size distribution exists in all the ZnO powders, with the bimodal peaks centering at 65–80 and 225–260 nm, respectively. Fig. 2(f) shows the particle size distribution of the sample $Zn_{0.96}Al_{0.04}O$ (nominal composition with 4 at% Al dopant concentration) as a typical example, with the two peaks centering at 80 and 260 nm, respectively.

The XRD results of the hot-pressed samples are shown in Fig. 3. The un-labeled diffraction peaks correspond to the ZnO phase. All the sintered samples contain mainly the ZnO phase. No alumina was detected in the sintered samples. There are no obvious differences between the XRD patterns obtained for pure ZnO and ZnO doped with 1 at% Al samples. However, when the Al dopant concentration increased to 2 and 4 at%, extra diffraction peaks corresponding to the $ZnAl_2O_4$ spinel phase appeared. The formation of the $ZnAl_2O_4$ is consistent with earlier reports that the solution limit of Al in ZnO is around 1 at%, and beyond this solution limit, the extra Al will not dissolve further into the ZnO lattice and $ZnAl_2O_4$ impurity phase will be formed [8].

The SEM images in Fig. 4 show the microstructure of the sintered ZnO samples. The result shows that a relatively dense sample with no significant grain growth can be achieved under the current sintering condition. The average grain size of the sintered samples was estimated from the SEM images using the linear intercept method [9]. The results are summarized in Table 1. The pure ZnO sample has an average grain size of ~2.52 μm. With the addition of 1 at% Al, the grain size decreases to ~1 μm. Further increase in Al dopant content

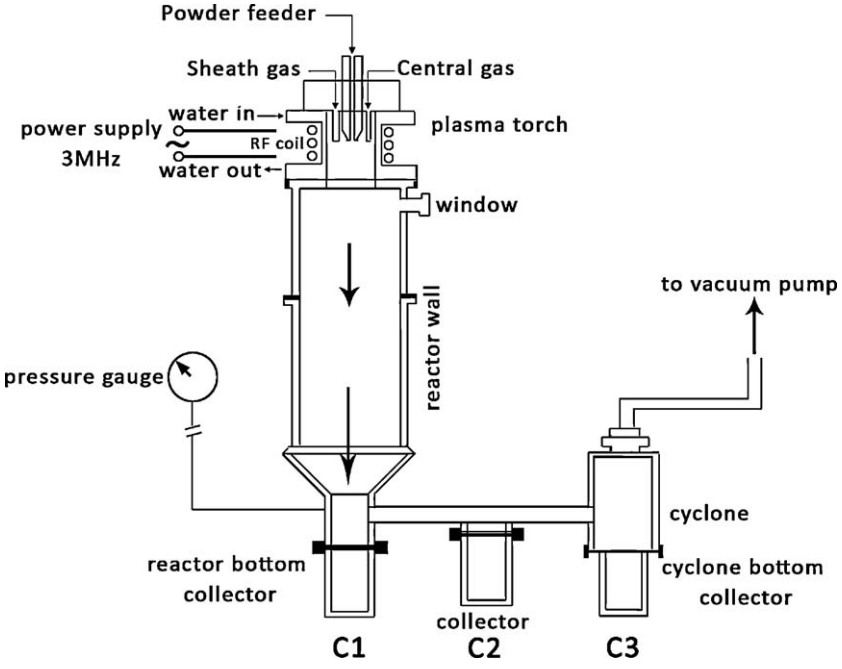

Fig. 1. A schematic view of the TEKNA induction RF Plasma System.

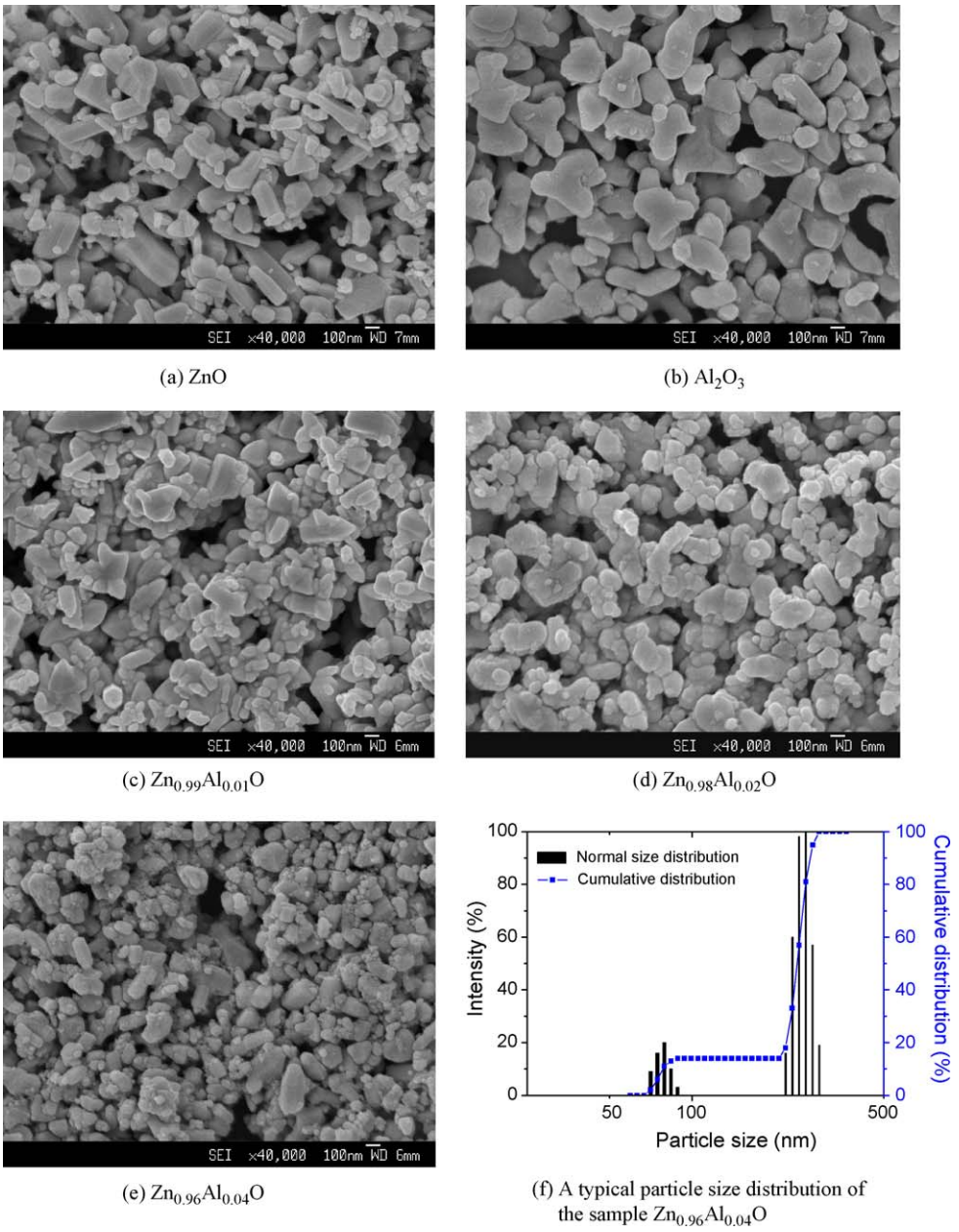

Fig. 2. The morphology (a)–(e) of the raw and plasma processed ZnO powders and a typical particle size distribution curve (f); (a) ZnO, (b) Al_2O_3, (c) $Zn_{0.99}Al_{0.01}O$, (d) $Zn_{0.98}Al_{0.02}O$, (e) $Zn_{0.96}Al_{0.04}O$, and (f) the particle size distribution curve of sample $Zn_{0.96}Al_{0.04}O$.

results in a further reduction in the average grain size to ~0.85–0.93 μm. The formation of $ZnAl_2O_4$ secondary phase may contribute to the prohibition of grain growth at higher Al doping level, which can restrict grain growth by blocking mass transportation and pinning the grain boundaries of the matrix materials [8,10].

Fig. 5(a) displays the electrical conductivity of the pure and Al-doped ZnO samples measured from 300 to 1100 K. All the doped samples exhibit metallic conductivity behavior. For example, a high electrical conductivity (~70,000 S/m) was obtained for the 1 at% Al-doped sample at room temperature. It is ~70 times higher than that obtained for the pure ZnO sample. The results indicate that the carrier concentration was significantly increased and the RF plasma processing is very effective in Al-doping. With further increase in Al dopant concentration from 2 to 4 at%, there is a slight decrease in the electrical conductivity. This decrease is due mainly to the increase in the amount of $ZnAl_2O_4$ spinel phase [11], which blocks and scatters electron transfer in the sintered sample. In addition, it has been reported that by increasing the doping level, hall mobility will be reduced and this can cause a reduction in the electrical conductivity, even without any significant change in the carrier concentration [12].

The temperature dependence of Seebeck coefficient for all the samples is shown in Fig. 5(b). Negative Seebeck coefficients are obtained for all the samples, indicating that the samples are all n-type. This is expected since the doping of Al^{3+} into the ZnO lattice will create extra electrons. It is

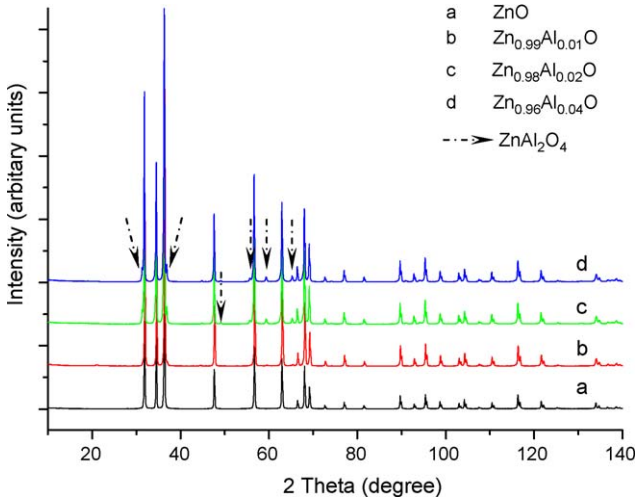

Fig. 3. XRD patterns of the hot-pressed ZnO samples.

observed that doping with Al significantly reduced the Seebeck coefficient by nearly one order of magnitude. One of the reasons for the reduction is related to the carrier concentration. A higher carrier concentration can cause a reduction in Seebeck coefficient S according to Eq. (1) [13]:

$$S = -\frac{k}{e}\left[\ln\frac{N_c}{n} + A\right] \quad (1)$$

Table 1
The grain size of the hot-pressed samples.

Sample	Grain size (μm)
ZnO	2.52
$Zn_{0.99}Al_{0.01}O$	1.03
$Zn_{0.98}Al_{0.02}O$	0.85
$Zn_{0.96}Al_{0.04}O$	0.93

where k is Boltzmann constant, e is the electron charge, N_c refers to the density of state, n denotes carrier concentration and A is a transport constant. Another possible reason to explain the reduction in Seebeck coefficient can be related to the hot pressing process used in this work. It has been reported that a much lower Seebeck coefficient was found in hot-pressed sample as compared to samples prepared by conventional sintering [7]. Such an observation may be due to the formation of defects when sintering is done in reduced atmosphere, which results in variation of carrier concentration. Thus, this will lead to an increase in conductivity and a reduction in Seebeck coefficient.

Fig. 5(c) shows the temperature dependence of the power factor f ($=S^2\sigma$) determined for the various samples. It is obvious that Al doping significantly improves the power factor at high temperatures. The power factors determined in the current study are comparable to the results reported in Al-doped ZnO prepared by other nanopowder processing techniques such as

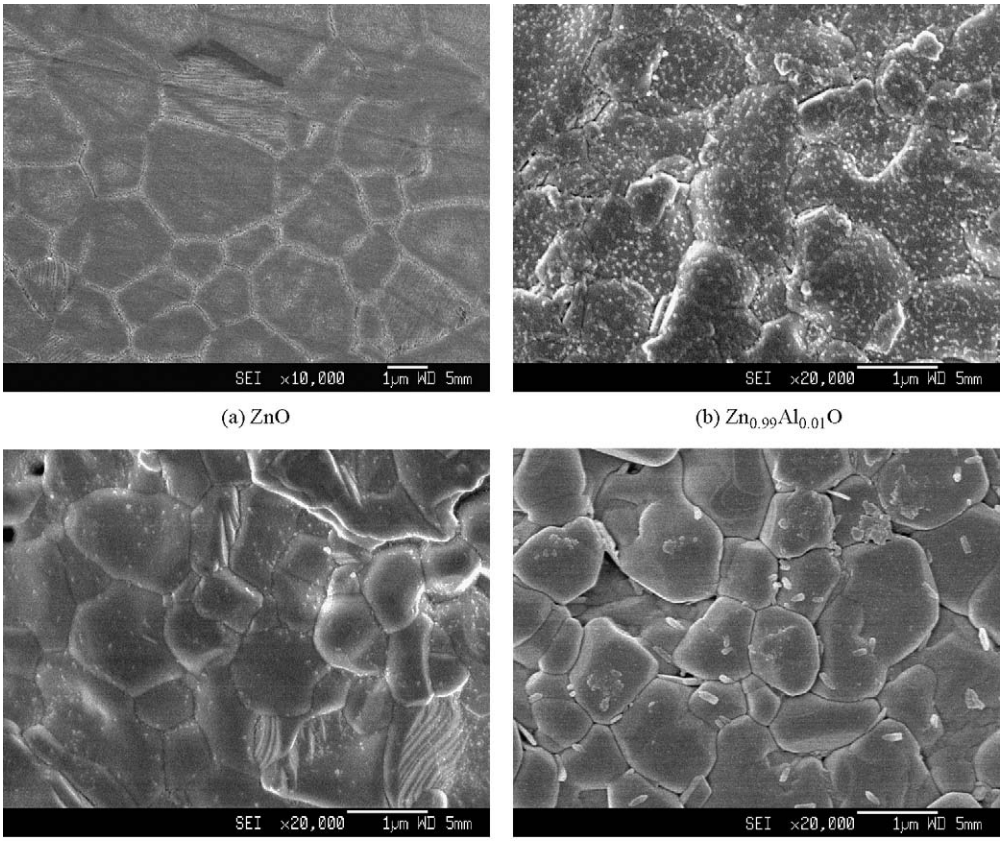

(a) ZnO (b) $Zn_{0.99}Al_{0.01}O$

(c) $Zn_{0.98}Al_{0.02}O$ (d) $Zn_{0.96}Al_{0.04}O$

Fig. 4. SEM microstructures of the hot-pressed ZnO samples; (a) ZnO, (b) $Zn_{0.99}Al_{0.01}O$, (c) $Zn_{0.98}Al_{0.02}O$, and (d) $Zn_{0.96}Al_{0.04}O$.

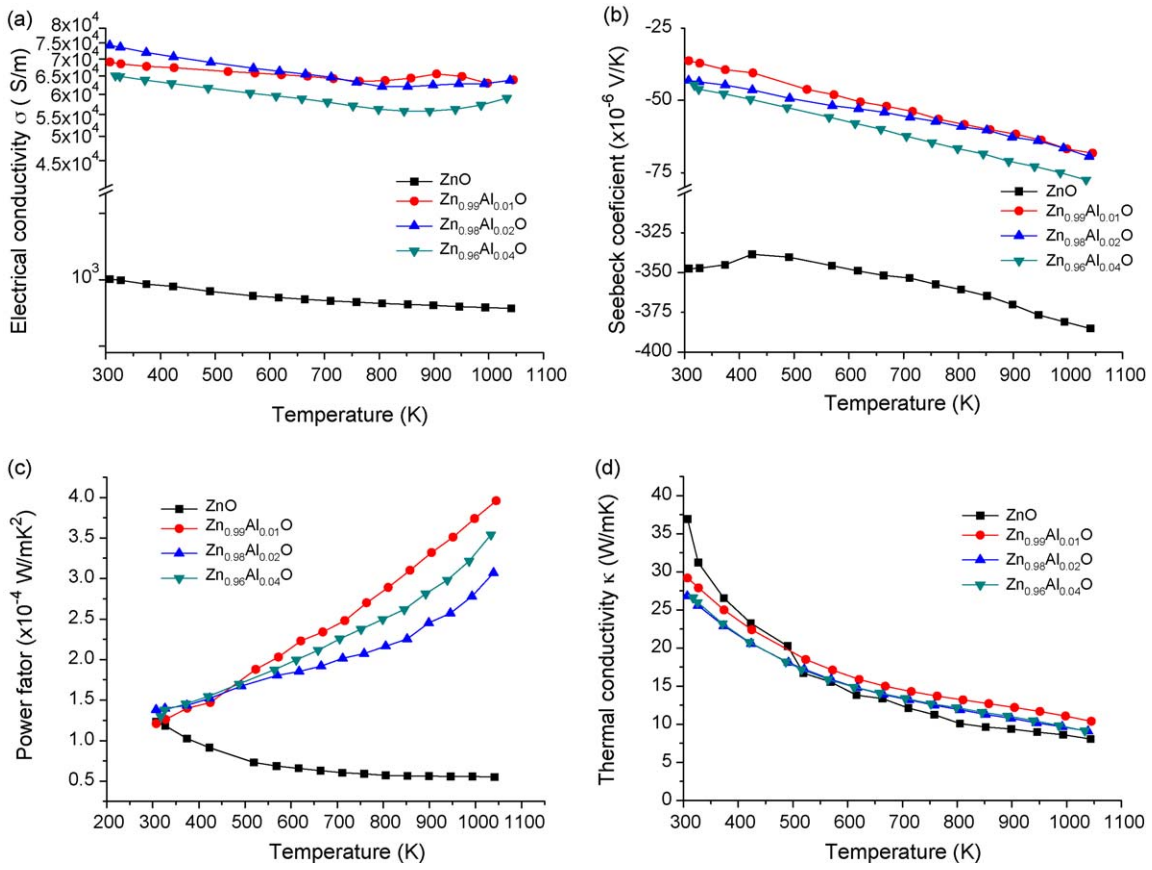

Fig. 5. Temperature dependence of the (a) electrical conductivity; (b) Seebeck coefficient; (c) power factor; and (d) thermal conductivity of the hot-pressed ZnO samples.

sol–gel and polymerized complex method [4,7,8]. Hence, the current results show that effective doping can be achieved by RF plasma processing.

The variation of thermal conductivity κ with temperature for the various samples is shown in Fig. 5(d). Due to its strong covalent bonding and light atoms, the wurtzite ZnO has a high intrinsic thermal conductivity. In bulk ZnO, the κ value can be as high as 100 W/m K [14]. With a small average grain size of ~2.52 μm, our pure ZnO sample still shows a relatively high thermal conductivity of ~37 W/m K at room temperature. This shows that the grain boundary scattering has limited effect to significantly reduce the thermal conductivity. Increasing the temperature steadily reduces the thermal conductivity as observed in both the doped and un-doped ZnO samples. A linear relationship can be found in the κ–$10^3/T$ curve, indicating that thermal conductivity is dominated by phonon transfer [12]. It is also noted that the thermal conductivity values of Al-doped samples are lower than the undoped sample only at low temperature. This agrees with the theoretical prediction that at low temperature, grain boundary and impurity scattering dominate phonon transfer and determine the final thermal conductivity [15]. With 1 at% Al doping, the amount of reduction in thermal conductivity (from 37 to 28 W/m K at room temperature) was not significant, which indicates that Al is not an effective atom for phonon scattering. A heavier dopant atom is necessary to suppress the lattice thermal conductivity of ZnO materials. At high temperature, the abnormal lower thermal conductivity of pure ZnO than the doped sample is not well understood and worth for further investigation.

Based on the results obtained for σ, S and κ, the dimensionless figure of merit ZT ($=\sigma S^2 T/\kappa$) are determined and presented in Fig. 6. The result shows that doping helps to

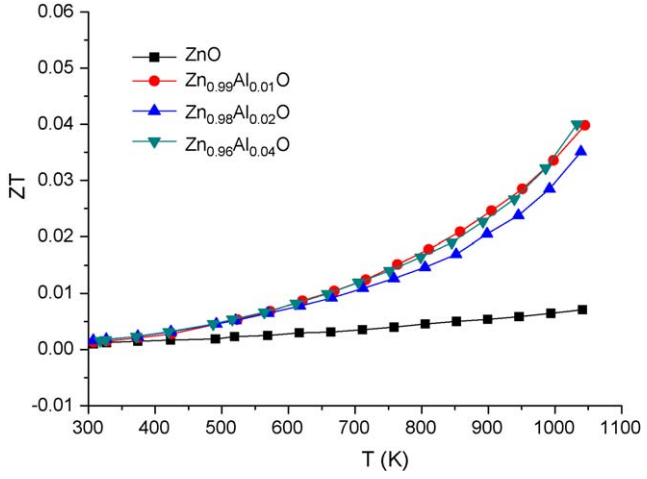

Fig. 6. Temperature dependence of the figure of merit ZT of the hot-pressed ZnO samples.

improve the ZT of ZnO materials, especially at high temperatures. Unfortunately, the very high thermal conductivity deteriorates the overall TE performance of the Al-doped ZnO samples. In order to improve the TE properties of ZnO-type materials, finding an efficient way to reduce the thermal conductivity of ZnO materials is as important as electronic doping. Co-doping ZnO with Al and other heavier impurity atoms is a potential approach that can be considered in future studies.

4. Conclusions

1–4 at% Al-doped ZnO nanopowder was prepared by RF plasma processing technique and sintered by hot press technique. The thermoelectric performance of the sintered samples was studied and discussed.

Metallic electrical conductivity was found in the doped samples, which shows that RF plasma processing technique can be effectively used in materials doping and in preparing nanostructured materials. The measured power factors are comparable to those reported in Al-doped ZnO prepared by other nanopowder processing techniques.

Even with a sub-micro-sized grain structure, high thermal conductivity was commonly found in all the samples prepared in this work, which significantly deteriorate the overall TE performance of the samples. Further research effort on effectively reducing the thermal conductivity is very necessary to fully explore the potential of this technique on preparing high performance thermoelectric materials.

Acknowledgement

The authors would like to thank Prof. Alfred Tok in the School of Materials Science & Engineering, Nanyang Technological University, Singapore for his support on using the RF Plasma System.

References

[1] D.M. Rowe (Ed.), Thermoelectrics Handbook: Macro to Nano, CRC Press, Taylor & Francis Group, Boca Raton, FL, 2006.
[2] K. Koumoto, I. Terasaki, R. Funahashi, Complex oxide materials for potential thermoelectric applications, MRS Bulletin 31 (2006) 206–210.
[3] X.F. Tang, H. Li, Q.J. Zhang, M. Niino, Ta. Goto, Synthesis and thermoelectric properties of double-atom-filled skutterudite compounds Ca_mCe_n-$Fe_xCo_{4-x}Sb_{12}$, Journal of Applied Physics 100. (2006), 123702-1-8.
[4] K.F. Cai, E. Müller, C. Drašar, A. Mrotzek, Preparation and thermoelectric properties of Al-doped ZnO ceramics, Materials Science & Engineering B 104 (2003) 45–48.
[5] M.S. Dresselhaus, G. Chen, M.Y. Tang, R.G. Yang, H. Lee, D.Z. Wang, Z.F. Ren, J.-P. Fleurial, P. Gogna, New directions for low-dimensional thermoelectric materials, Advanced Materials 19 (2007) 1043–1053.
[6] B.A. Cook, J.L. Harring, C.B. Vining, Electrical properties of Ga and ZnS doped ZnO prepared by mechanical alloying, Journal of Applied Physics 83 (1998) 5858–5861.
[7] Y. Fujishiro, M. Miyata, M. Awano, K. Maeda, Effect of microstructural control on thermoelectric properties of hot-pressed aluminum-doped zinc oxide, Journal of American Ceramic Society 86 (2003) 2063–2066.
[8] S. Katsuyama, Y. Takagi, M. Ito, K. Majima, H. Nagai, H. Sakai, K. Yoshimura, K. Kosuge, Thermoelectric properties of $(Zn_{1-y}Mg_y)_{1-x}Al_xO$ ceramics prepared by the polymerized complex method, Journal of Applied Physics 92 (2002) 1391–1398.
[9] J.C. Wurst, J.A. Nelson, Lineal intercept technique for measuring grain size in two-phase polycrystalline ceramics, Journal of American Ceramic Society 55 (1972) 109.
[10] K.H. Kim, S.H. Shim, K.B. Shim, K. Niihara, J. Hojo, Microstructural and thermoelectric characteristics of zinc oxide-based thermoelectric materials fabricated using a spark plasma sintering process, Journal of American Ceramic Society 88 (2005) 628–632.
[11] K. Park, K.Y. Ko, Effect of TiO_2 on high-temperature thermoelectric properties of ZnO, Journal of Alloys and Compounds 430 (2007) 200–204.
[12] M. Ohtaki, T. Tsubota, K. Eguchi, Thermoelectric properties of oxide solid solutions based on Al-doped ZnO, in: Proceedings ICT98, 17th International Conference on Thermoelectrics, 1998, pp. 610–613.
[13] Y. Kinemuchi, C. Ito, H. Kaga, T. Aoki, K. Watari, Thermoelectricity of Al-doped ZnO at different carrier concentrations, Journal of Materials Research 22 (2007) 1942–1946.
[14] Ü. Özgür, Ya.I. Alivov, C. Liu, A. Teke, M.A. Reshchikov, S. Doğan, V. Avrutin, S.J. Cho, H. Morkoç, A comprehensive review of ZnO materials and devices, Journal of Applied Physics 98 (2005), 041301-1-103.
[15] R. Berman, Thermal Conduction in Solids, Clarendon Press, Oxford, 1976